Journal of Magnetism and Magnetic Materials 573 (2023) 170674

Contents lists available at ScienceDirect

Journal of Magnetism and Magnetic Materials

journal homepage: www.elsevier.com/locate/jmmm

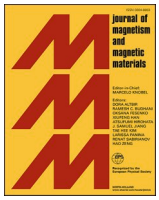

Control of coexistent phase by rotation of magnetic field in a metamagnetic FeRh thin film

Yali Xie [a], Baomin Wang [b,*], Lei Zhang [c], Xinming Wang [d], Huali Yang [a], Gengfei Li [a], Run-Wei Li [a,e,*]

[a] CAS Key Laboratory of Magnetic Materials and Devices and Zhejiang Province Key Laboratory of Magnetic Materials and Application Technology, Ningbo Institute of Materials Technology and Engineering, Chinese Academy of Sciences, Ningbo 315201, People's Republic of China
[b] School of Physical Science and Technology, Ningbo University, Ningbo 315211, People's Republic of China
[c] Anhui Key Laboratory of Condensed Matter Physics at Extreme Conditions, High Magnetic Field Laboratory, Chinese Academy of Sciences, Hefei 230031, People's Republic of China
[d] Analytical Center, Ningbo Institute of Materials Technology and Engineering, Chinese Academy of Sciences, Ningbo 315201, People's Republic of China
[e] Center of Materials Science and Optoelectronics Engineering, University of Chinese Academy of Sciences, Beijing 100049, People's Republic of China

ARTICLE INFO

Keywords:
Coexistent phase
FeRh thin film
Rotation of magnetic field

ABSTRACT

Here, we report the change of the FM and AF coexistent state in a MPTM FeRh thin film by simply rotating of the magnetic field. We find that the resistance of the coexistent phase can be changed by up to 19% by the rotation of the magnetic field. This kind of resistance change is obviously different from the usual anisotropic magnetoresistance in metallic materials whether in the angle-dependent behavior or in the magnitude. These results show another way to control the FM-AF coexistent phase, which determines the multifunctional properties of the MPTMs.

1. Introduction

Magnetic materials having a large change in the saturation magnetization during the phase transition are usually known as metamagnetic phase transition materials (MPTMs)[1,2]. Owing to the different electrical and magnetic properties of the materials before and after a phase transition, several interesting phenomena, such as a giant magnetoresistance effect [3,4], giant magnetocaloric effect [5-8], barocaloric effect [9], and heat-assisted or electrically assisted magnetic recording [10,11], have been observed around the metamagnetic phase transition. The key features of these materials around the phase transition are metastability and phase-coexistence [2]. According to the Clausius–Clapeyron relation, the phase transition temperature between two metastable phases can be changed by the magnitude of magnetic field. The values of the phase transition temperature can also be changed for measuring along different directions of the sample owing to the intrinsic anisotropy of the crystal lattice [12-14]. The two phases before and after the metamagnetic phase transition coexist in the phase transition region [15,16]. The resistance and magnetization of the coexistent phase is in monotonous proportion to the value of the temperature at a fixed magnetic field or the magnitude of the magnetic field at a fixed temperature, giving the fraction of field-induced phase represented by $F(H, T)$. Owing to the first-order characteristic of the metamagnetic phase transition, $F(H, T)$ further evolves with time [17,18]. Usually, the $F(H, T)$ increases slowly (decreases quickly) over time in a superheated (SH) (supercooled (SC)) state. Consequently, the fraction of the field-induced phase can be further defined as $F(H, T, t)$.

Metamagnetic FeRh thin film undergoes a peculiar first-order phase transition from antiferromagnetic (AF) phase at room temperature to ferromagnetic (FM) phase upon heating above the transition temperature [19,20]. Due to this magnetic transition, FeRh thin films have attracted wide attentions for their potential applications in magnetic storage [10,21], magnetic refrigeration [7,22], and so on [23-25]. In order to realize these potential applications of FeRh thin film, many effort has been utilize to control the phase transition by different external field, such as strain [26,27], optical pulses [28,29], electric field [30,31], and magnetic field [32]. Here, we report the effect of the magnetic field direction on the $F(H, T, t)$ of the coexistent phase in a metamagnetic FeRh epitaxial thin film. We find an irreversible resistance change that can reach up to 19% with a magnetic field rotated out-of-plane at the FM and AF coexistent state, demonstrating that the direction of the applied magnetic field can tune the fraction of field-

* Corresponding authors.
E-mail addresses: wangbaomin@nbu.edu.cn (B. Wang), runweili@nimte.ac.cn (R.-W. Li).

https://doi.org/10.1016/j.jmmm.2023.170674
Received 8 December 2022; Received in revised form 8 March 2023; Accepted 25 March 2023
Available online 29 March 2023

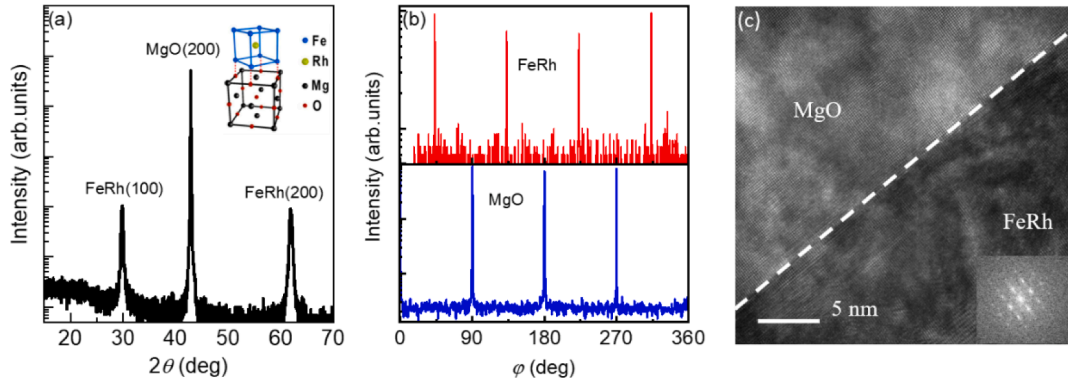

Fig. 1. The crystal structure of FeRh/MgO. (a) XRD pattern of FeRh/MgO. The inset shows the growth model of the FeRh film on the MgO substrates. (b) X-ray φ-scans and (c) HRTEM and FFT images of FeRh/MgO.

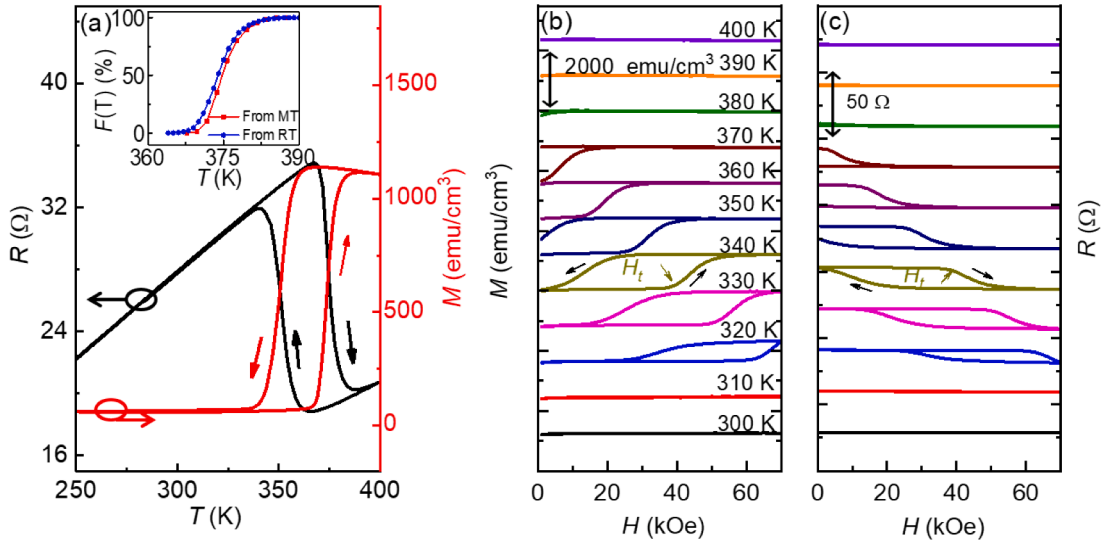

Fig. 2. The metamagnetic phase transition of FeRh film. (a) Temperature dependence of resistance and magnetization for the FeRh film measured at 0 kOe and 2 kOe, respectively. The inset shows the temperature dependence of *F*(T) obtained from the temperature dependence of magnetization (MT) and the temperature dependence of resistance (RT), respectively. (b) Magnetic field dependence of magnetization for FeRh thin film at different temperatures. (c) Magnetic field dependence of resistance for FeRh thin film at different temperatures. The field sweeps were taken at temperature steps starting at 300 K.

induced FM phase further.

2. Experimental

Epitaxial 30-nm thick equiatomic FeRh thin films were deposited on commercial (1 0 0)-oriented MgO substrates in a magnetron sputtering system with a base pressure of below 1.0×10^{-8} Torr. Prior to deposition, the substrates were annealed at 530 °C for 1 h in a vacuum chamber. The film was grown at a temperature of 530 °C and then annealed at 670 °C for 1 h. The film thicknesses were controlled based on the deposition time, which was calibrated through X-ray reflectivity (XRR). The epitaxial growth of the FeRh film was characterized by in-plane X-ray φ-scans using XRD. The microstructure of the FeRh film was observed by high-resolution transmission electron microscopy (HRTEM). Transport and magnetotransport were carried out using a physical property measurement system (PPMS, Quantum Design) equipped with a motorized sample rotator and a standard four-probe contact for the resistance measurements. The magnetic properties were measured using a Quantum Design superconducting quantum interference device-vibrating sample magnetometer (SQUID-VSM).

3. Results

3.1. Epitaxial growth of the FeRh film

Fig. 1a shows the X-ray diffractometer (XRD) θ-2θ pattern of the FeRh/MgO sample. The strong XRD peaks indicate the high quality of the FeRh film with the FeRh (1 0 0) surface parallel to the surface of the MgO (1 0 0) substrates. The X-ray φ-scans with a fixed 2θ value at the (0 1 1) reflection display a 90° interval of four peaks. The FeRh peaks are observed at 45° with respect to the MgO peaks, which indicate that the FeRh film is epitaxially grown with a 45° in-plane structure rotation on the MgO (1 0 0) substrate (Fig. 1b), as shown in the inset of Fig. 1a. A typical cross-sectional HRTEM image and a corresponding fast Fourier transform (FFT) image further confirm the epitaxial growth of the FeRh film (Fig. 1c).

3.2. Metamagnetic phase transition of FeRh film

The phase transition of the FeRh film was investigated by both magnetization and transport measurements, as shown in Fig. 2a. The magnetization measurements were carried out with in-plane magnetic field of 2 kOe applied along MgO [0 0 1] direction, whereas transport measurements were carried out under no magnetic field. The

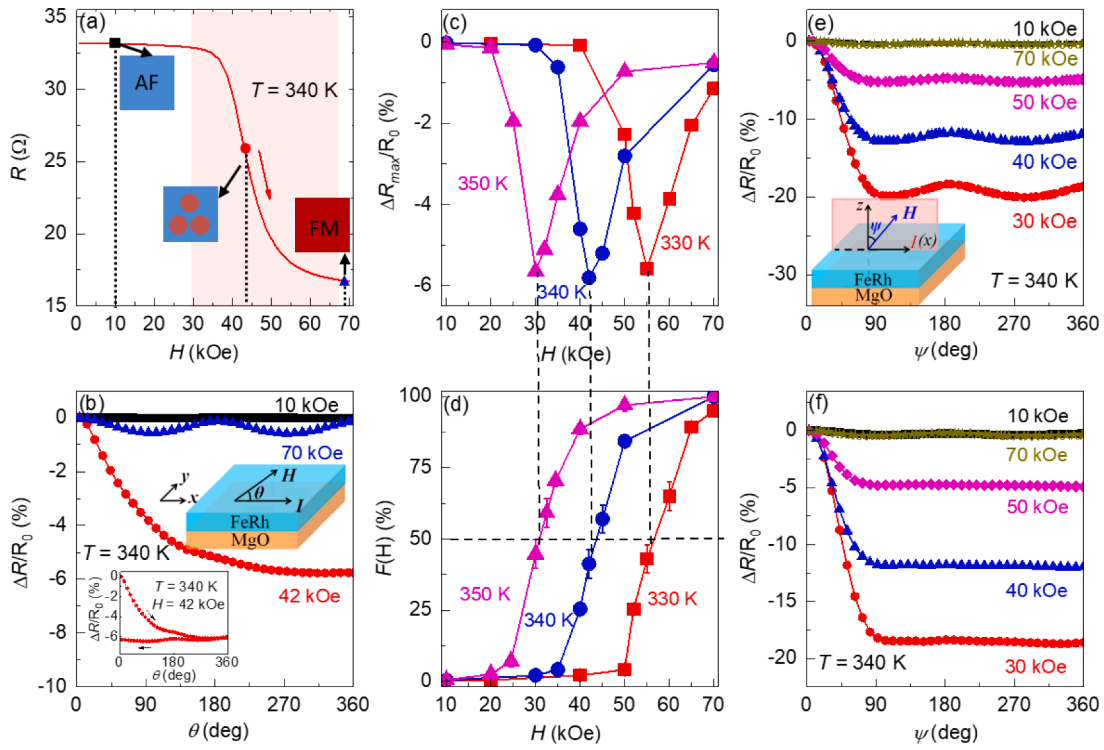

Fig. 3. Angle-dependent magnetoresistance. (a) The magnetic field dependent resistance of FeRh thin film measured at 340 K. The shadow region shows the phase-coexistent state. (b) Angle-dependent resistance change in FeRh thin film measured at 340 K under in-plane magnetic fields of 10, 42, and 70 kOe, respectively. The inset in the right corner shows the measurement configuration with magnetic field rotated in-plane. The inset in the left corner shows the repeated measurement of the angle-dependent resistivity in FeRh thin film at 340 K under in-plane magnetic fields of 42 kOe. (c) Magnetic field dependence of maximum change in resistance at 330 K, 340 K, and 350 K. (d) Magnetic field dependence of F(H) at 330 K, 340 K, and 350 K. (e) Angle-dependent resistance change in FeRh thin film measured at 340 K under out-of-plane magnetic fields of 10, 30, 40, 50, and 70 kOe, respectively. The inset shows the measurement configuration with the magnetic field rotated out-of-plane. (f) The corresponding changes in angle-dependent resistance after subtracting the normal AMR effect.

magnetization of the FeRh film increased from approximately 50 emu/cm^3 at room temperature to 1120 emu/cm^3 at 390 K during the heating process, indicating a typical metamagnetic phase transition of FeRh. The possible origin of magnetization in the AF phase at room temperature has been proposed, such as substrate strain, changing composition, symmetry breaking, or topography of FeRh thin film [15,33,34]. During the cooling process, the magnetization of the FeRh film gradually decreases to the initial value with a remarkable temperature hysteresis, indicating the first-order characteristic of the phase transition, which is consistent with previous reports [19,32]. Meanwhile, the resistance decreased from approximately 33.2 Ω at 370 K to 19.0 Ω at 390 K during the heating process, and then gradually changed to its initial value during the cooling process, confirming the first-order phase transition above room temperature. Under the phase-coexistent state, the magnetization and resistance are in monotonous proportion to the temperature, indicating that F(T) can be represented by both magnetization and resistance. The total resistance of the FeRh thin film can be considered to be the sum of the resistances of the AF and FM parts. Thus, the entire resistance R can be written as $R = R_{FM} \times F + R_{AF} \times (1 - F)$, where F is the volume fraction of the FM phase, and R_{FM} and R_{AF} are the resistivities for the FM and AF states, respectively [35]. According to this equation, the temperature dependence of F(T) can be obtained from the temperature-dependent resistance during the heating process. Similarly, it can also be obtained from the temperature-dependent magnetization. The calculated temperature dependence of F(T) is shown in the inset of Fig. 2a. The applied 2 kOe magnetic field in the temperature dependent magnetization measurement process decrease the phase transition temperature, leading to the offset of the MT and RT curve. According to the same method used above, the relative F(H) can also be calculated from the isothermal magnetic field dependence of the resistance. Fig. 2b displays the magnetic field dependence of magnetization for the FeRh thin film at different temperatures with the magnetic field applied in the plane. Before each measurement, the sample was first decreased to 300 K to ensure the same starting state and then increased to the target temperatures. The magnetization remains almost unchanged as the applied magnetic field increases below 320 K (AF state) and above 380 K (FM state). When the temperature is between 320 and 380 K, an increase in the magnetization can be observed at the transition field (H_t), indicating the occurrence of the field-induced metamagnetic phase transition. The magnetic field dependence of the resistance of the FeRh thin film shows a similar behavior (Fig. 2c). The change in magnetization and resistance is due to the change in F(H, T) during the field-induced metamagnetic phase transition. Meanwhile, it can be seen that the field-induced metamagnetic phase transition behavior can be observed more clearly at 340 K, so we take it as an example to study the control of coexistent phase by rotation of magnetic field in the following study.

3.3. Angle-dependent magnetoresistance

Fig. 3a shows the resistance versus in-plane magnetic field at 340 K. When the applied magnetic field $H < 30$ kOe and > 68 kOe, the FeRh thin film is in AF and FM states, respectively. When $30 < H < 68$ kOe, the FeRh thin film is in a phase-coexistent state (the shadow region), during which the FM and AF phases coexist. Fig. 3b shows the angle-dependent resistance change measured at 340 K with in-plane magnetic fields of 10 kOe (AF state), 42 kOe (phase-coexistent state), and 70 kOe (FM state), respectively. The measurement setup is shown schematically in the insets of Fig. 3b. To eliminate the temporal evolution effect, the magnetic field was applied for 0.5 h before the resistance measurements, and then the effect of field-induced shift of the resistance is negligible. The resistance change is $\triangle R/R_0 = [R(\theta) - R(0)]/R(0)$, where $R(\theta)$ is the resistance with the magnetic field applied along the direction at which

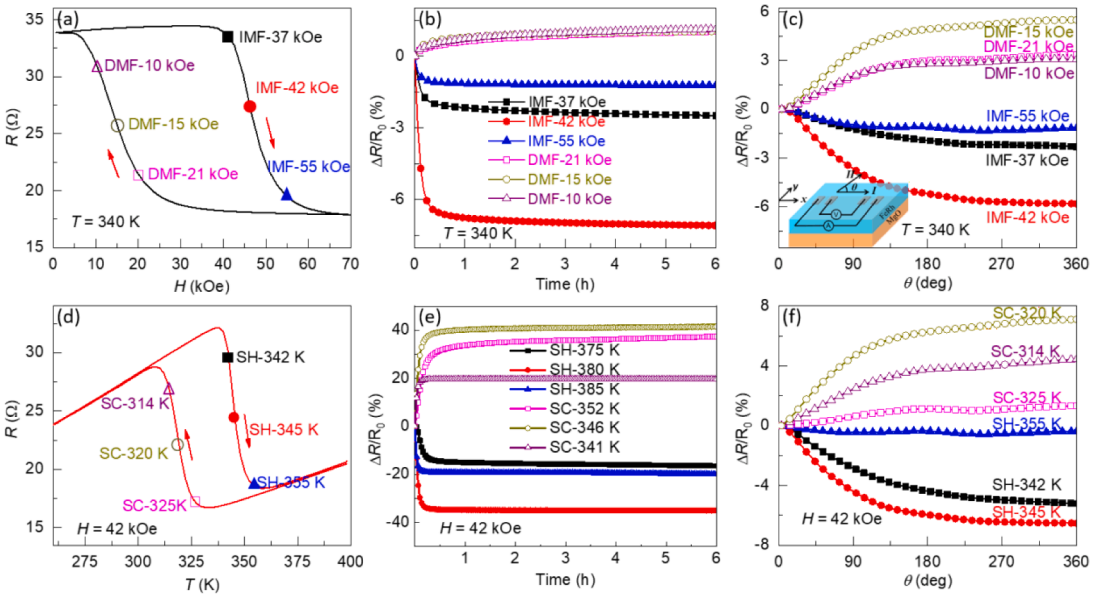

Fig. 4. Angle-dependent magnetoresistance at different phase-coexistent states. (a) Magnetic field dependence of resistances for FeRh thin film at 340 K. The red arrows represent the processes of the magnetic field change. (b) The temporal evolution effect in FeRh thin film measured at 340 K with different magnetic fields applied under different IMF and DMF states. (c) The angle-dependent resistance change measured under different IMF and DMF states after 6 h of relaxation. The inset shows the measurement configuration with magnetic field rotated in-plane. (d) Temperature-dependence of resistance in FeRh thin film measured under 42 kOe magnetic field. The red arrows represent the processes of the temperature change. (e) The temporal evolution effect in FeRh thin film measured at different temperature with 42 kOe magnetic fields applied under different SH and SC states. (f) The angle-dependent resistance change measured under different SH and SC states after 6 h of relaxation. (For interpretation of the references to colour in this figure legend, the reader is referred to the web version of this article.)

the angle between magnetic field direction and current direction is θ, and $R(0)$ is the resistance with the magnetic field applied along the x-axis. Under a FM-AF coexistent state (H = 42 kOe), $\triangle R/R_0$ has an irreversible decrease accompanying the rotation of the magnetic field, which can reach approximately 6%, showing a vector feature of F(H). As a comparison, an irreversible decrease in resistance disappeared at both AF (H = 10 kOe) and FM states (H = 70 kOe). Under an FM state, the angle-dependent $\triangle R/R_0$ follows a $\cos^2\theta$ angular dependence, originating from the anisotropic magnetoresistance (AMR) in FM materials [36]. The irreversible resistance change behavior disappear during the subsequent back-and-forth angular scans of θ between 0° and 360°, which ultimately recovers the symmetric oscillatory behavior of normal AMR effect (the inset of Fig. 3b).

Fig. 3c summarizes the $\triangle R_{max}/R_0$ values measured at 330, 340, and 350 K. At 340 K, the magnetic field-dependent $\triangle R_{max}/R_0$ shows a valley at 42 kOe, where the FeRh thin film is under a coexistent FM-AF state. At 330 and 350 K, the magnetic field-dependent $\triangle R_{max}/R_0$ shows a similar behavior to that of 340 K. Compared with the results obtained at 340 K, the valley of $\triangle R_{max}/R_0$ is obtained in larger (55 kOe) and smaller (30 kOe) fields at lower (330 K) and higher (350 K) temperatures, respectively. Fig. 3d shows the magnetic field dependences of F(H) at 330, 340, and 350 K. It can be found that the valley of $\triangle R_{max}/R_0$ always appears at the magnetic field amplitude, where F(H, T) is approximately 50%, demonstrating that the angle-dependent change in resistance under a consistent FM-AF state has a strong relationship with F(H, T) of the FM phase.

Fig. 3e shows the angle-dependent resistance measured at 340 K with out-of-plane magnetic fields of 10, 30, 40, 50, and 70 kOe, respectively. The measurement configuration is shown in the inset of Fig. 3e. The magnetic field was applied out-of-plane with angle ψ relative to the z direction. Under FM-AF coexistent states (H = 30, 40, and 50 kOe), an unusual angle-dependent resistance change can also be observed. Fig. 3f shows the angle-dependent resistance change after subtracting the normal AMR with $\cos^2\theta$ dependence. The resistance change accompanying the rotation of the magnetic field reaches up to 19% at H = 30 kOe. When the magnetic field rotates out of plane, it is inevitable to consider the influence of demagnetization field. Due to our measurements were conducted in the coexisting phase, the influence of the demagnetization field is relatively small, which is similar to that observed in perovskite manganites [37]. Thus, the angle-dependent resistance change cannot be explained solely by the demagnetization field effect.

3.4. Angle-dependent magnetoresistance at different phase-coexistent states

The above measured phase-coexistent states are obtained by increasing the magnetic field (defined as the IMF state). To investigate this effect under different states, we also performed measurements under coexistent FM-AF states obtained by decreasing the magnetic field (defined as a DMF state), by increasing the temperature (defined as the SH state), and by a temperature decrease (defined as the SC state). To obtain each IMF state, the magnetic field was increased from zero to the target magnetic field at a constant temperature. To obtain each DMF state, the magnetic field was first increased from zero to 70 kOe, and then decreased to the target magnetic field at a constant temperature, all the measurement are carried out with in-plane magnetic fields. Fig. 4a shows the magnetic field dependent resistances of the FeRh thin film at 340 K. The red arrows represent the processes of change in the magnetic field. Fig. 4b shows the temporal evolution effect in the FeRh thin film measured at 340 K with different magnetic fields applied under the IMF and DMF states. At the half-way during the IMF phase transition process (IMF-42 kOe), the resistance decreases with time. However, it tends to be saturated approximately 0.5 h later. The temporal evolution effect of the magnetic field-induced coexistent phase is similar to that induced by temperature during the first-order phase transition [17,18].When the measurement magnetic field is IMF-37 kOe (IMF-55 kOe), at which the phase transition will begin (finished), the change in resistance becomes lower than that of IMF-42 kOe. During the DMF phase transition process, a similar behavior to that in the IMF phase transition process is shown, except that the resistance increases with a temporal evolution, demonstrating that the temporal evolution effect can enhance the F(H) under

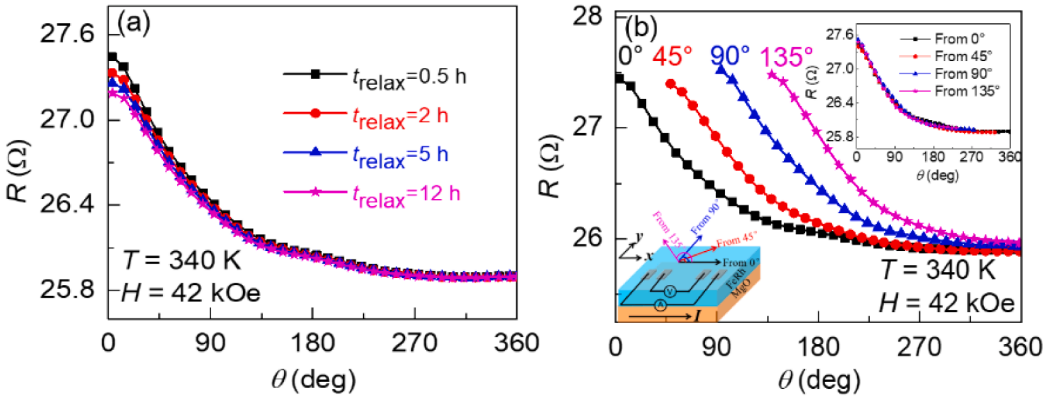

Fig. 5. The basic properties of the angle-dependent magnetoresistance at 340 K. (a) The angle-dependent resistances at 340 K measured after relaxing for different periods of time (t_{relax} = 0.5, 2, 5, 12 h) under in-plane magnetic field of 42 kOe. (b) Angle-dependent resistance in FeRh thin film measured at 340 K under in-plane magnetic field of 42 kOe along different initial directions. The inset in the left corner shows the measurement configuration with magnetic field applied from different initial directions. The inset in the right corner shows the angle-dependent resistance, which is normalized to zero degrees.

the IMF state while reducing it under the DMF state. Fig. 4c shows the angle-dependent resistance change of magnetic field-induced coexistent phases at both the IMF and DMF states. All the resistances were measured after 6 h relaxation to reduce the temporal evolution effect. The measurement setup is shown schematically in the insets of Fig. 4c. It can be seen that an irreversible change ratio in resistance can reach approximately 6% accompanying the rotation of the magnetic field at both the IMF and DMF states. The resistance decreases with the rotation of the magnetic field at the IMF state, indicating an increase in *F*(H). Meanwhile, it increases at the DMF state, indicating that the rotation of the magnetic field reduces *F*(H).

Fig. 4d shows the process of realizing different SH and SC states. To obtain each SH state, the temperature was increased from 250 K to the target temperature. To obtain each SC state, the temperature was first increased from 250 to 400 K, and then decreased to the target temperature. Fig. 4e shows temporal evolution effect in FeRh thin film measured at different temperature in the SH and SC states. It shows the similar behaviors with that in the IMF and DMF states except the larger resistance change ratio. Fig. 4f shows the change in the angle-dependent resistance under different SH and SC states. An irreversible change ratio in resistance can reach approximately 6% accompanying the rotation of the magnetic field at both the SH and SC states can also be observed. The resistance decreases in the SH state while it increases in the SC state accompanied by a rotation of the magnetic field, indicating that the direction of change in the magnetic field can enhance the *F*(T) under the SH state while reducing it under the SC state.

4. Discussion and conclusion

The irreversible resistance change behavior accompanying the rotation of the magnetic field is similar to that observed in strongly correlated manganite, which may come from the preferential expansion of the volume of FM domains in the field applied direction [38]. During the angular sweep, by a continuous sweeping of the magnetic field direction in the film plane, the overall volume of FM phase is increased and the resistivity is decreased. However, this mechanism is not suitable for FeRh thin film, because the resistance in FeRh thin film increases when rotating the magnetic field (Fig. 4c), indicating that the rotation of the magnetic field reduces field-induced FM phase.

In order to further rule out the temporal evolution effect on the angle-dependent resistance change, we measured the angle-dependent resistance after relaxing for different periods of time (t_{relax} = 0.5, 2.0, 5.0, 12.0 h, Fig. 5a). Both the behavior and the resistance change ratio are unchanged, which indicates that the temporal evolution effect is not the origin of the angle-dependent resistance change behavior. To eliminate the effect of the anisotropy of the crystal lattice [12-14], the angle-dependent resistance was measured starting from different directions. The measurement configuration, which indicates the starting directions, is shown in the inset of Fig. 5b (left corner). All the resistances were measured after 0.5 h relaxation to reduce the temporal evolution effect. The irreversible decreases in resistance accompanying the rotation of the magnetic field show similar behaviors for different starting directions. When these angle-dependent resistances were normalized to zero, the starting direction irrelevant behavior was clearly observed (inset of Fig. 5b, right corner), indicating that the angle-dependent resistance change has no relationship with the anisotropy of the FeRh crystal lattice.

To summarize, we studied the effect of the magnetic field direction on the FM-AF coexistent state in FeRh thin films. The rotation of the magnetic field can tune the resistance change ratio of the coexistent magnetic phase by up to 19%. Moreover, the angle-dependent change ratio in resistance has a strong relationship with *F*(H, T) of the FM phase. Although the mechanism of control of coexistent phase by rotation of magnetic field still needs to be studied theoretically and experimentally, our present results have already demonstrated another way to control the multifunctional properties of MPTMs by rotation of magnetic field, and may promote the application of MPTMs based on the tunable FM-AF coexistent state.

CRediT authorship contribution statement

Yali Xie: Investigation, Formal analysis, Writing – original draft. **Baomin Wang:** Conceptualization, Writing – review & editing, Supervision, Funding acquisition. **Lei Zhang:** Investigation. **Xinming Wang:** Investigation. **Huali Yang:** Formal analysis. **Gengfei Li:** Investigation. **Run-Wei Li:** Supervision, Funding acquisition.

Declaration of Competing Interest

The authors declare that they have no known competing financial interests or personal relationships that could have appeared to influence the work reported in this paper.

Data availability

No data was used for the research described in the article.

Acknowledgements

We acknowledge the financial support from the National Natural

Science Foundation of China (No. 51931011, 52127803, 51971233, 92064011, 62174164), the K. C. Wong Education Foundation (No. GJTD-2020-11), "Pioneer" and "Leading Goose" R&D Program of Zhejiang (2022C01032), the Ningbo Science and Technology Bureau (Grant No. 2022Z086, 2022Z094).

References

[1] E. Stryjewski, N. Giordano, Metamagnetism, Adv. Phys. 26 (5) (1977) 487–650, https://doi.org/10.1080/00018737700101433.
[2] S. B. Roy, P. Chaddah, V. K. Pecharsky, K. A. Gschneidner Jr., Overview No. 145 Metamagnetic transitions, phase coexistence and metastability in functional magnetic materials, Acta Mater. 56 (20), (2008) 5895–5906, https://doi.org/10.1016/j.actamat.2008.08.040.
[3] V.L. Moruzzi, P.M. Marcus, Giant magnetoresistance in FeRh: A natural magnetic multilayer, Phys. Rev. B 46 (21) (1992) 14198–14200, https://doi.org/10.1103/PhysRevB.46.14198.
[4] S.Y. Yu, Z.H. Liu, G.D. Liu, J.L. Chen, Z.X. Cao, G.H. Wu, Large magnetoresistance in single-crystalline $Ni_{50}Mn_{50-x}In_x$ alloys (x=14–16) upon martensitic transformation, Appl. Phys. Lett. 89 (16) (2006), 162503, https://doi.org/10.1063/1.2362581.
[5] V.K. Pecharsky, K.A. Gschneidner Jr., Giant Magnetocaloric Effect in $Gd_5(Si_2Ge_2)$, Phys. Rev. Lett. 78 (23) (1997) 4494, https://doi.org/10.1103/PhysRevLett.78.4494.
[6] T. Krenke, E. Duman, M. Acet, E.F. Wassermann, X. Moya, L. Mañosa, A. Planes, Inverse magnetocaloric effect in ferromagnetic Ni-Mn-Sn alloys, Nat. Mater. 4 (6) (2005) 450–454, https://doi.org/10.1038/nmat1395.
[7] Y. Liu, L.C. Phillips, R. Mattana, M. Bibes, A. Barthélémy, B. Dkhil, Large reversible caloric effect in FeRh thin films via a dual-stimulus multicaloric cycle, Nat. Commun. 7 (1) (2016) 11614, https://doi.org/10.1038/ncomms11614.
[8] B.F. Lu, J. Liu, Mechanocaloric materials for solid-state cooling, Sci. Bull. 60 (19) (2015) 1638–1643, https://doi.org/10.1007/s11434-015-0898-5.
[9] L. Manosa, D. Gonzalez-Alonso, A. Planes, E. Bonnot, M. Barrio, J.L. Tamarit, S. Aksoy, M. Acet, Giant solid-state barocaloric effect in the Ni–Mn–In magnetic shape-memory alloy, Nat. Mater. 9 (6) (2010) 478–481, https://doi.org/10.1038/nmat2731.
[10] J.-U. Thiele, S. Maat, E.E. Fullerton, FeRh/FePt exchange spring films for thermally assisted magnetic recording media, Appl. Phys. Lett. 82 (17) (2003) 2859, https://doi.org/10.1063/1.1571232.
[11] R.O. Cherifi, V. Ivanovskaya, L.C. Phillips, A. Zobelli, I.C. Infante, E. Jacquet, V. Garcia, S. Fusil, P.R. Briddon, N. Guiblin, A. Mougin, A.A. Ünal, F. Kronast, S. Valencia, B. Dkhil, A. Barthélémy, M. Bibes, Electric-field control of magnetic order above room temperature, Nat. Mater. 13 (4) (2014) 345–351, https://doi.org/10.1038/nmat3870.
[12] H. Tang, V.K. Pecharsky, G.D. Samolyuk, M. Zou, K.A. Gschneidner Jr., V. P. Antropov, D.L. Schlagel, T.A. Lograsso, Anisotropy of the Magnetoresistance in $Gd_5Si_2Ge_2$, Phys. Rev. Lett. 93 (23) (2004), 237203, https://doi.org/10.1103/PhysRevLett.93.237203.
[13] M. Zou, Ya. Mudryk, V. K. Pecharsky, K. A. Gschneidner, Jr., D. L. Schlagel, T. A. Lograsso, Crystallography, anisotropic metamagnetism, and magnetocaloric effect in $Tb_5Si_{2.2}Ge_{1.8}$, Phys. Rev. B 75(2), (2007) 024418, https://doi.org/10.1103/PhysRevB.75.024418.
[14] F.F. Baldis, M. Sirena, L.B. Steren, V.H. Etgens, M. Eddrief, C. Ulysse, G. Faini, Anisotropic magnetic-field-induced phase transition in MnAs nanoribbons, Appl. Phys. Lett. 107 (1) (2015), 012407, https://doi.org/10.1063/1.4926567.
[15] C. Gatel, B. Warot-Fonrose, N. Biziere, L.A. Rodríguez, D. Reyes, R. Cours, M. Castiella, M.J. Casanove, Inhomogeneous spatial distribution of the magnetic transition in an iron-rhodium thin film, Nat. Commun. 8 (1) (2017) 15703, https://doi.org/10.1038/ncomms15703.
[16] Y.D. Wang, E.W. Huang, Y. Ren, Z.H. Nie, G. Wang, Y.D. Liu, J.N. Deng, H. Choo, P. K. Liaw, D.E. Brown, L. Zuo, In situ high-energy X-ray studies of magnetic-field-induced phase transition in a ferromagnetic shape memory Ni–Co–Mn–In alloy, Acta Mater. 56 (4) (2008) 913–923, https://doi.org/10.1016/j.actamat.2007.10.045.
[17] M. Manekar, S. B. Roy, Nucleation and growth dynamics across the antiferromagnetic to ferromagnetic transition in $(Fe_{0.975}Ni_{0.025})_{50}Rh_{50}$: analogy with crystallization, J. Phys. Condens. Matter. 20(32), (2008) 325208, https://doi.org/10.1088/0953-8984/20/32/325208.
[18] B. M. Wang, L. Wang, Y. Liu, B. C. Zhao, Y. Zhao, Y. Yang, H. Zhang, Strong thermal-history-dependent magnetoresistance behavior in $Ni_{49.5}Mn_{34.5}In_{16}$, J. Appl. Phys. 106(6), (2009) 063909, https://doi.org/10.1063/1.3225578.
[19] L. Muldawer, F. de Bergevin, Antiferromagnetic-Ferromagnetic Transformation in FeRh, J. Chem. Phys. 35 (5) (1961) 1904–1905, https://doi.org/10.1063/1.1732175.
[20] J.S. Kouvel, C.C. Hartelius, Anomalous Magnetic Moments and Transformations in the Ordered Alloy FeRh, J. Appl. Phys. 33 (3) (1962) 1343, https://doi.org/10.1063/1.1728721.
[21] N.T. Nam, W. Lu, T. Suzuki, Exchange bias of ferromagnetic/antiferromagnetic in FePt/FeRh bilayers, J. Appl. Phys. 105 (7) (2009) 07D708, https://doi.org/10.1063/1.3062813.
[22] Q. B. Hu, J. Li, C. C. Wang, Z. J. Zhou, Q. Q. Cao, T. J. Zhou, D. H. Wang, Y. W. Du, Electric field tuning of magnetocaloric effect in $FeRh_{0.96}Pd_{0.04}$/PMN-PT composite near room temperature, Appl. Phys. Lett. 110(22), (2017) 222408, https://doi.org/10.1063/1.4984901.
[23] Y.Y. Wang, M.M. Decker, T.N.G. Meier, X.Z. Chen, C. Song, T. Grünbaum, W. S. Zhao, J.Y. Zhang, L. Chen, C.H. Back, Spin pumping during the antiferromagnetic–ferromagnetic phase transition of iron–rhodium, Nat. Commun. 11 (1) (2020) 275, https://doi.org/10.1038/s41467-019-14061-w.
[24] X. Marti, I. Fina, C. Frontera, J. Liu, P. Wadley, Q. He, R.J. Paull, J.D. Clarkson, J. Kudrnovský, I. Turek, J. Kuneš, D. Yi, J.-H. Chu, C.T. Nelson, L. You, E. Arenholz, S. Salahuddin, J. Fontcuberta, T. Jungwirth, R. Ramesh, Room-temperature antiferromagnetic memory resistor, Nat. Mater. 13 (4) (2014) 367–374, https://doi.org/10.1038/nmat3861.
[25] T. Nan, Y. Lee, S. Zhuang, Z. Hu, J.D. Clarkson, X. Wang, C. Ko, H. Choe, Z. Chen, D. Budil, J. Wu, S. Salahuddin, J. Hu, R. Ramesh, N. Sun, Electric-field control of spin dynamics during magnetic phase transitions, Sci. Adv. 6 (40) (2020) eabd2613, https://doi.org/10.1126/sciadv.abd2613.
[26] I. Suzuki, M. Itoh, T. Taniyama, Elastically controlled magnetic phase transition in Ga-FeRh/$BaTiO_3$(001) heterostructure, Appl. Phys. Lett. 104 (2) (2014), 022401, https://doi.org/10.1063/1.4861455.
[27] Y.L. Xie, Q.F. Zhan, T. Shang, H.L. Yang, B.M. Wang, J. Tang, R.W. Li, Effect of epitaxial strain and lattice mismatch on magnetic and transport behaviors in metamagnetic FeRh thin films, AIP Adv. 7 (5) (2017), 056314, https://doi.org/10.1063/1.4976301.
[28] G. Ju, J. Hohlfeld, B. Bergman, R. J. M. van deVeerdonk, O. N. Mryasov, J.-Y. Kim, X. Wu, D. Weller, B. Koopmans, Ultrafast Generation of Ferromagnetic Order via a Laser-Induced Phase Transformation in FeRh Thin Films, Phys. Rev. Lett. 93(19), (2004) 197403, https://doi.org/10.1103/PhysRevLett.93.197403.
[29] A.B. Mei, I. Gray, Y. Tang, J. Schubert, D. Werder, J. Bartell, D.C. Ralph, G. D. Fuchs, D.G. Schlom, Local Photothermal Control of Phase Transitions for On-Demand Room-Temperature Rewritable Magnetic Patterning, Adv. Mater. 32 (22) (2020) 2001080, https://doi.org/10.1002/adma.202001080.
[30] I. Fina, N. Dix, E. Menéndez, A. Crespi, M. Foerster, L. Aballe, F. Sánchez, J. Fontcuberta, Flexible Antiferromagnetic FeRh Tapes as Memory Elements, ACS Appl. Mater. Inter. 12 (13) (2020) 15389–15395, https://doi.org/10.1021/acsami.0c00704.
[31] Y. Lee, Z.Q. Liu, J.T. Heron, J.D. Clarkson, J. Hong, C. Ko, M.D. Biegalski, U. Aschauer, S.L. Hsu, M.E. Nowakowski, J. Wu, H.M. Christen, S. Salahuddin, J. B. Bokor, N.A. Spaldin, D.G. Schlom, R. Ramesh, Large resistivity modulation in mixed-phase metallic systems, Nat. Commun. 6 (1) (2015) 5959, https://doi.org/10.1038/ncomms6959.
[32] S. Maat, J.-U. Thiele, E.E. Fullerton, Temperature and field hysteresis of the antiferromagnetic-to-ferromagnetic phase transition in epitaxial FeRh films, Phys. Rev. B 72 (21) (2005), 214432, https://doi.org/10.1103/PhysRevB.72.214432.
[33] C. Bull, C.W. Barton, W. Griggs, A. Caruana, C.J. Kinane, P.W. Nutter, T. Thomson, PNR study of the phase transition in FeRh thin film, APL Mater. 7 (10) (2019), 101117, https://doi.org/10.1063/1.5120622.
[34] W. Griggs, B. Eggert, M.O. Liedke, M. Butterling, A. Wagner, U. Kentsch, E. Hirschmann, M. Grimes, A.J. Caruana, C. Kinane, H. Wende, R. Bali, T. Thomson, Depth selective magnetic phase coexistence in FeRh thin films, APL Mater. 8 (12) (2020), 121103, https://doi.org/10.1063/5.0032130.
[35] G. Li, H.-D. Zhou, S.J. Feng, X.-J. Fan, X.-G. Li, Z.D. Wang, Competition between ferromagnetic metallic and paramagnetic insulating phases in manganites, J. Appl. Phys. 92 (3) (2002) 1406–1410, https://doi.org/10.1063/1.1490153.
[36] T. McGuire, R. Potter, Anisotropic magnetoresistance in ferromagnetic 3d alloys, IEEE Trans. Magn. 11 (4) (1975) 1018–1038, https://doi.org/10.1109/TMAG.1975.1058782.
[37] H. L. Yang, B. M. Wang, Y. W. Liu, Z. H. Yang, X. J. Zhu, Y. L. Xie, Z. H. Zuo, B. Chen,Q. F. Zhan, J. L. Wang, and R-W. Li. Unusual anisotropic magnetoresistance in charge-orbital ordered $Nd_{0.5}Sr_{0.5}MnO_3$ polycrystals. J. Appl. Phys. 116(23), (2014) 234505, https://doi.org/10.1063/1.4904437.
[38] H. S. Alagoz, J. Jeon, S. T. Mahmud, M. M. Saber, B. Prasad, M. Egilmez, K. H. Chow, J. Jung, Recovery of oscillatory magneto-resistance in phase separated $La_{0.3}Pr_{0.4}Ca_{0.3}MnO_3$ epitaxial thin films, Appl. Phys. Lett. 103(23), (2013) 232402, https://doi.org/10.1063/1.4839536.